Lunar Domes near Maraldi D: a preliminary report

By Raffaello Lena, Maximilian Teodorescu and Jim Phillips

Important clusters of lunar domes are observed in the Hortensius/Milichius/T. Mayer region in Mare Insularum and in Mare Tranquillitatis around the craters Arago and Cauchy [1-6]. A first map of the Cauchy shield was performed based on our previous works [4, 7-14] and describes morphometric properties of forty-eight domes, termed C1-C33, Vi1-8, D (Diana) and NTA1-NTA6. In this contribution we provide an analysis of further eight lunar domes detected using CCD telescopic image and located principally near Maraldi D, in the northern region of the Cauchy shield. We term the examined lunar domes, previously not introduced and described in our map, as C35-C42 (Fig.1 and Table 1). The examined domes described in the current article (Table 1) are reported in red label. Some domes have already been measured in previous studies [4, 7-14] and are reported in brackets. In the LRO WAC imagery the examined domes are not as prominent as in the telescopic CCD image taken under lower solar illumination angle.

Ground-based observations

A telescopic CCD image of the examined lunar region, near the crater Maraldi D, is shown in Fig. 1.

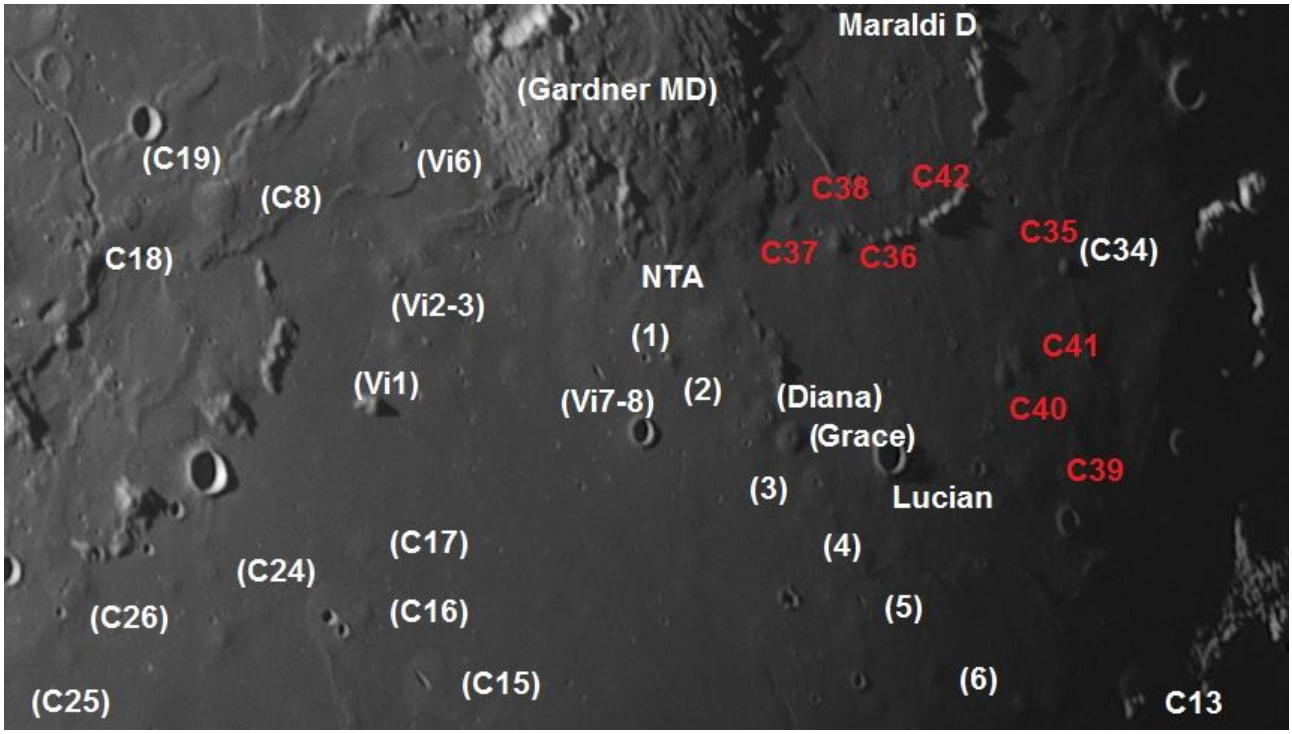

Figure 1: Telescopic CCD image made on December 16, 2019 at 00:44 UT by Teodorescu. Crop of the original image. The identified domes are marked in red (C35-C42).

Domes	Latitude (°)	Longitude (°)	Diameter (km)	h (m)	slope (°)	Volume Km^3	Class
C35	16.01	37.52	7.0 ± 0.3	45 ± 5	0.73 ± 0.1	0.86	A
C36	15.62	36.04	5.7 ± 0.3	120 ± 10	2.3 ± 0.2	1.4	$A\text{-}C_2\text{-}E_1$
C37	15.60	35.60	3.6 ± 0.3	70 ± 10	2.2 ± 0.2	0.36	$A\text{-}E_1$
C38	15.80	35.52	7.0 ± 0.3	95 ±10	1.5 ± 0.1	1.8	$A\text{-}C_2$
C39	14.51	38.02	12.0 ± 0.3	65 ± 10	0.62 ± 0.06	3.7	$A\text{-}C_2$
C40	15.15	37.68	4.8 ± 0.3	80 ± 10	2.0 ± 0.2	0.7	$C_2\text{-}E_1$
C41	15.27	37.79	9.8 ± 0.3	70 ± 10	0.82 ± 0.1	2.6	C_1
C42	16.13	36.49	6.4 ± 0.3	55 ± 5	0.98 ± 0.1	0.9	$A\text{-}C_2$

Table 1: Morphometric properties of the examined domes.

Digital elevation map based on telescopic CCD imagery

Generating an elevation map of a part of the lunar surface requires its three-dimensional (3D) reconstruction. A well-known image-based method for 3D surface reconstruction is shape from shading (SfS). It makes use of the fact that surface parts inclined towards the light source appear brighter than surface parts inclined away from it. The SfS approach aims for deriving the orientation of the surface at each image location by using a model of the reflectance properties of the surface and knowledge about the illumination conditions, finally leading to an elevation value for each image pixel [15]. The SfS method requires accurate knowledge of the scattering properties of the surface in terms of the bidirectional reflectance distribution function (BRDF).

The height h of a dome was obtained by measuring the altitude difference in the reconstructed 3D profile between the dome summit and the surrounding surface, considering the curvature of the lunar surface [4]. The average flank slope ζ was determined according to: $\zeta = \arctan 2h/D$.

The uncertainty results in a relative standard error of the dome height h of ±10 percent, which is independent of the height value itself. The dome diameter D can be measured at an accuracy of ± 5 percent. The 3D reconstructions of C35-C42 are shown in Fig. 2.

Further images of the wide Cauchy domes region are shown in Figs. 4-7.

Likely further domes of low profile may be present in this region, but new images are necessary in order to confirm suspected bumps (at the present unverified).

LOLA DEM

ACT-REACT Quick Map tool was used to access to the LOLA DEM dataset, allowing to obtain the cross-sectional profiles for the examined domes (Fig. 3).

Note the agreement of the measurements carried out on the CCD telescopic image and the LOLA DEM.

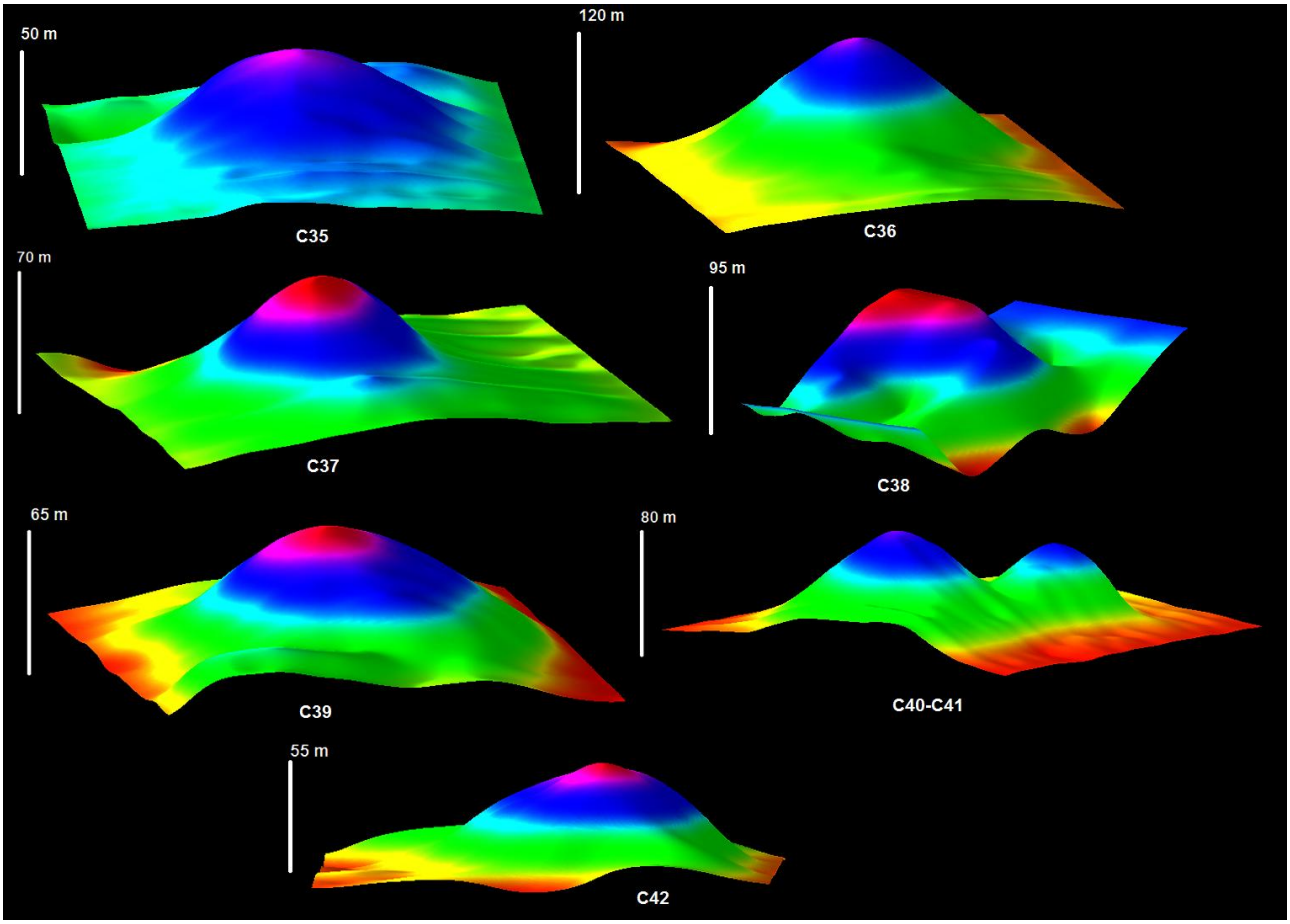

Figure 2: 3D reconstructions of C35-C42 based on terrestrial CCD image of Fig. 1 by photoclinometry and SfS analysis. The vertical axis is 20 times exaggerated.

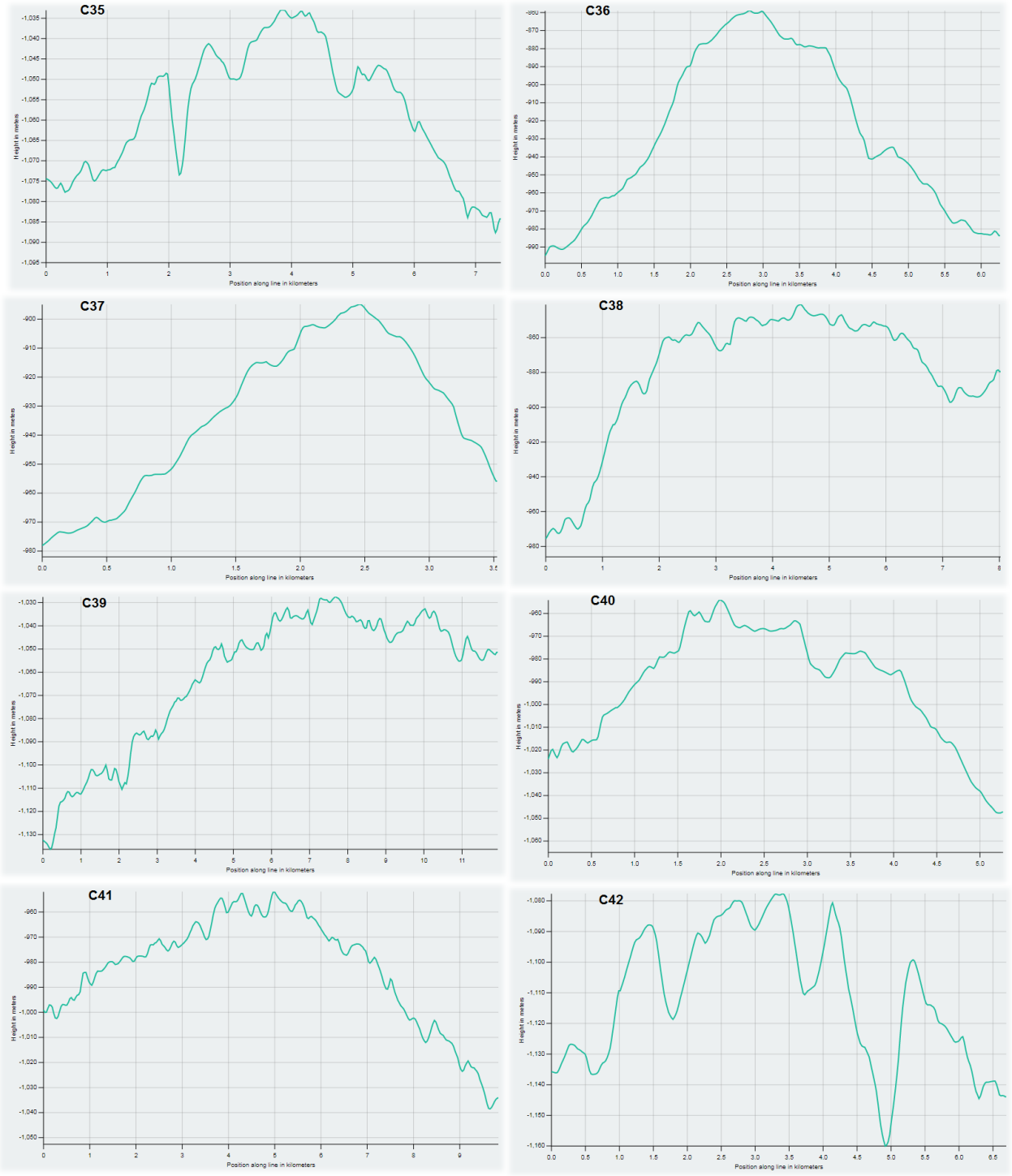

Figure 3: LRO WAC-derived surface elevation plot of C35-C42 based on LOLA DEM.

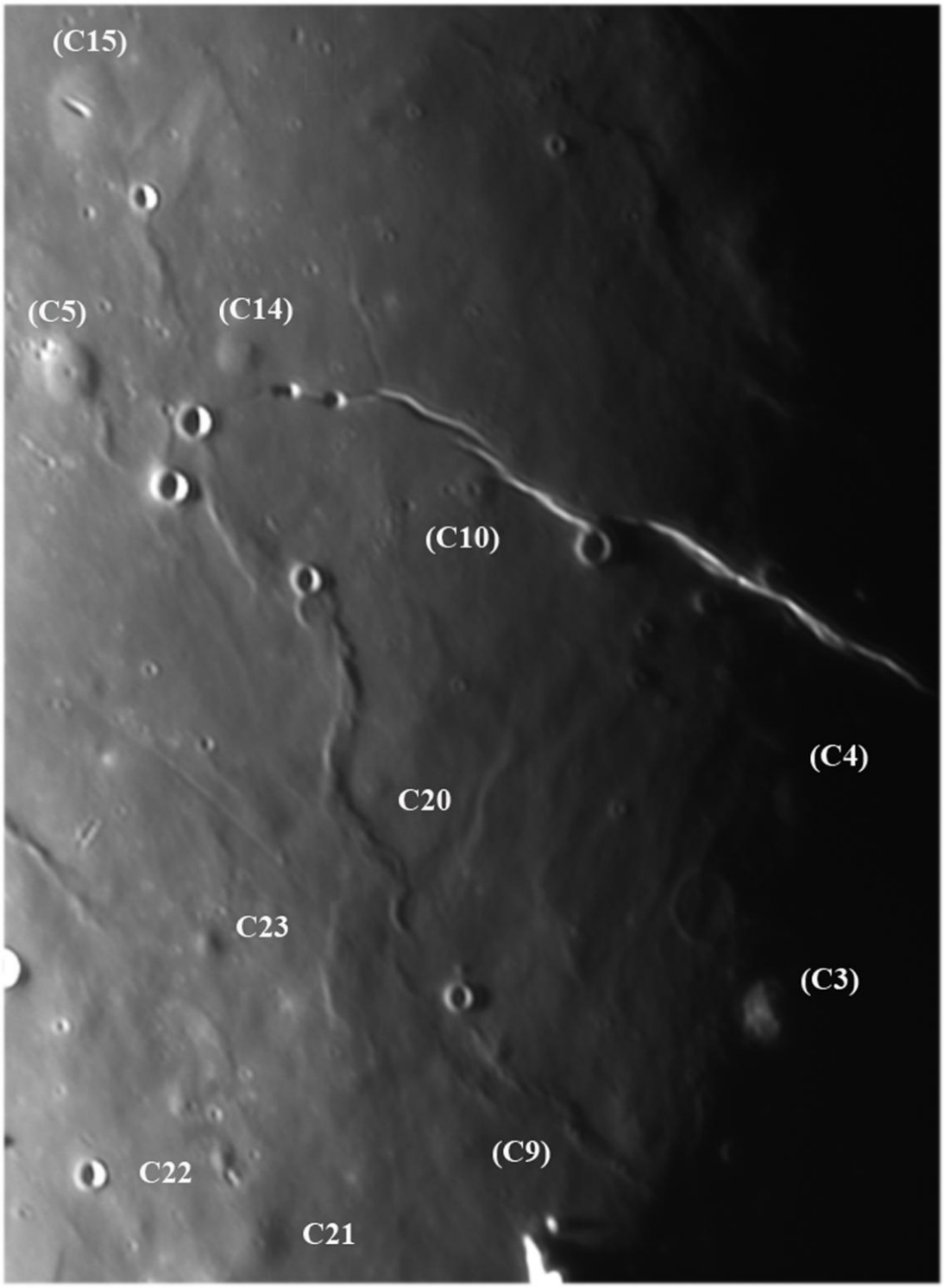

Figure 4: Examined lunar region (quadrant 1). Image made by Phillips on October 20, 2016 at 10:09 UT using an AP 10" (254mm) F/14.6 Maksutov telescope.

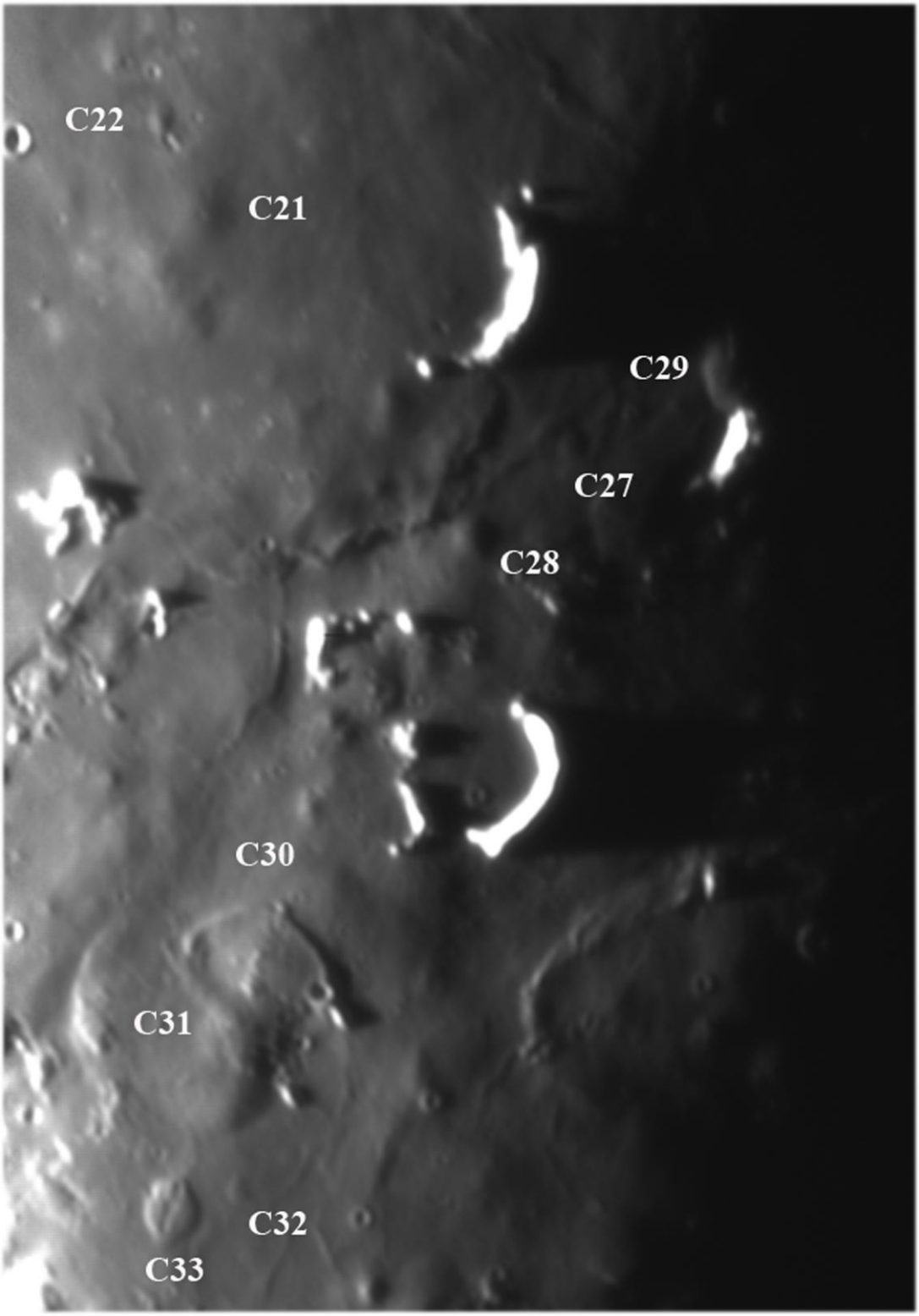

Figure 5: Examined lunar region (quadrant 2). Image made by Phillips on October 20, 2016 at 10:04 UT using an AP 10" (254mm) F/14.6 Maksutov telescope.

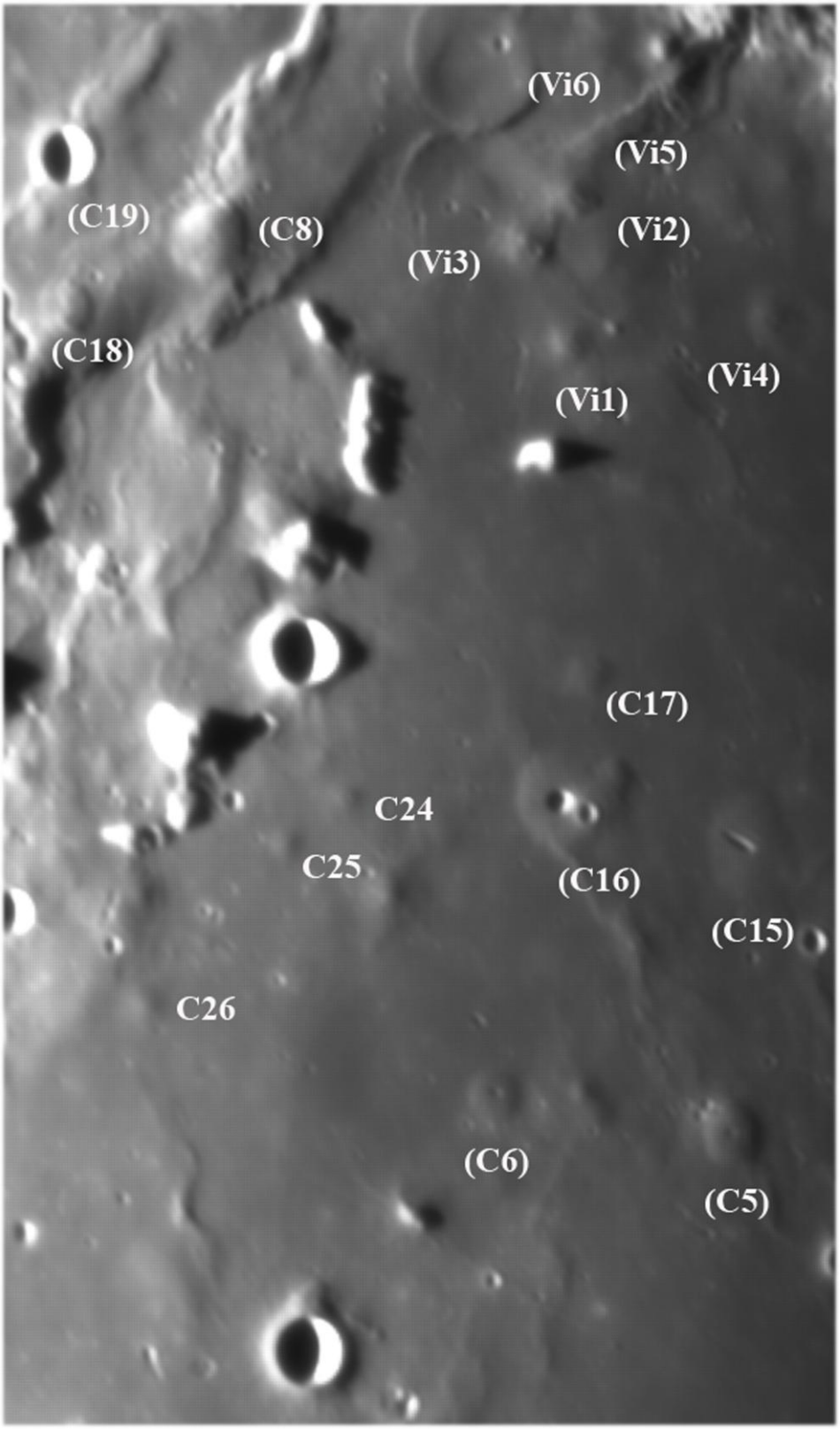

Figure 6: Examined lunar region (quadrant 3). Image made by Phillips on October 20, 2016 at 10:19 UT using an AP 10" (254mm) F/14.6 Maksutov telescope.

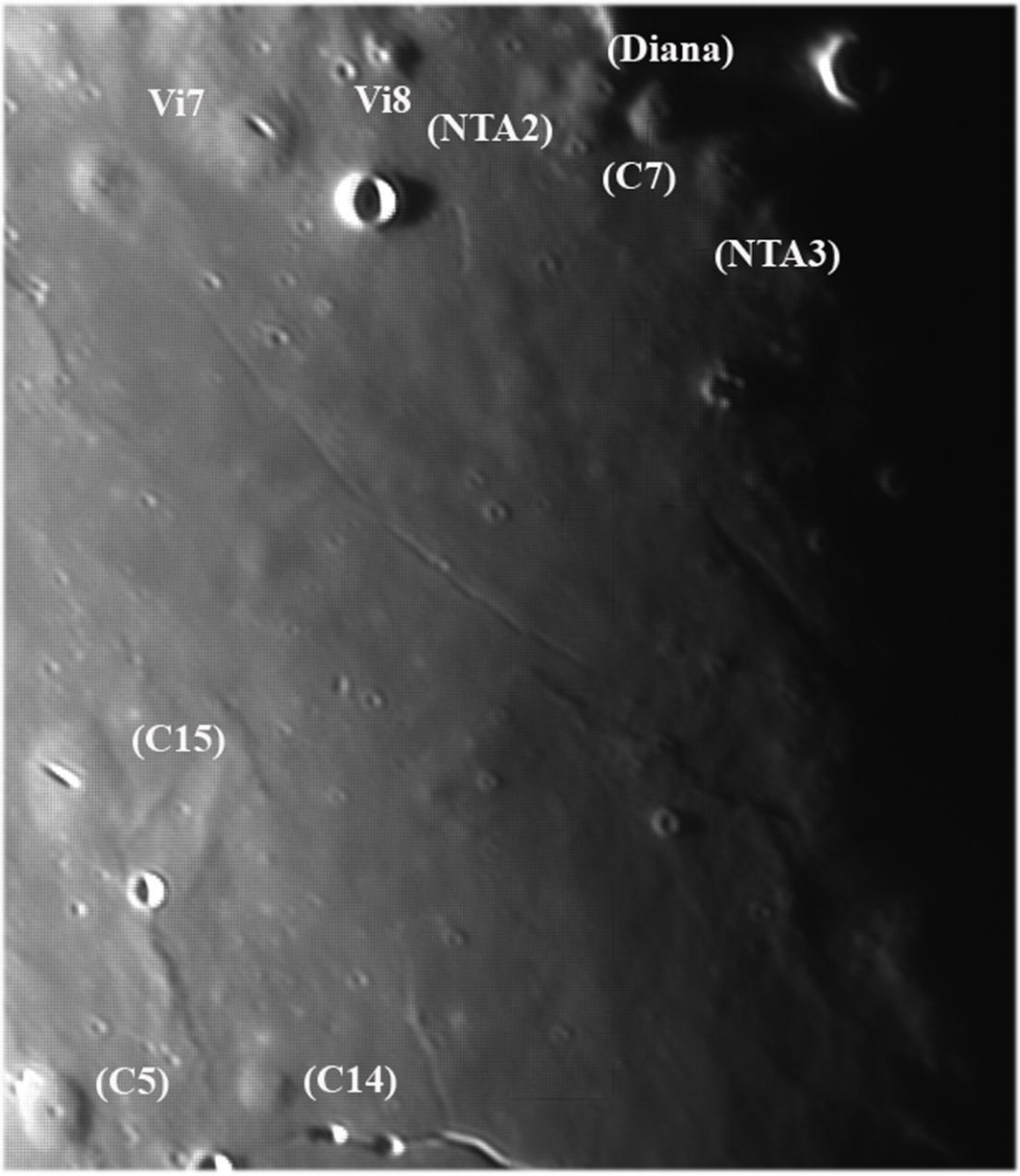

Figure 7: Examined lunar region (quadrant 4). Image made by Phillips on October 20, 2016 at 10:15 UT using an AP 10" (254mm) F/14.6 Maksutov telescope.

Results and discussion

Based on the spectral and morphometric data obtained in this study, C41belongs to class C_1, while the dome C35 belong to class A. The other domes belong to class A-C_2 or are intermediates belonging to class A-C_2-E_1, A-E_1 and C_2-E_1.

They span a continuous range of properties from spectrally blue (class A) to red (class E) soils and from very low (class A) to steep (class E_1) or shallow (class E_2) flank slopes. The class E domes represent the smallest volcanic edifices formed by effusive mechanisms observed to date. Domes of class C_2 are characterized by gentle flank slopes, moderate volumes which are higher than those of class A. They originate from moderately viscous lavas between 10^4 and 10^7 Pa s. The corresponding effusion rates between 100 and 300 $m^3 s^{-1}$ are comparable to those estimated for the class A domes, but the class C_2 domes were formed over longer periods of time between about 0.8 and 5 years.

Diviner Lunar Radiometer Experiment and Christiansen Feature (CF)

The Lunar Reconnaissance Orbiter's (LRO) Diviner Lunar Radiometer Experiment (spatial resolution of 950 m/pixel) produces thermal emissivity data, and provide compositional

information from three wavelengths centered around 8 μm that are used to characterize the Christiansen Feature (CF), which is directly sensitive to silicate mineralogy and the bulk SiO_2 content. These spectral bandpass filters are centered at 7.00, 8.25, and 8.55 μm. The major minerals of lunar soils- plagioclase, pyroxene, and olivine- have different ranges of CF values [16]. The feldspar and high silicic material, including quartz, silica-rich glass, and alkali and ternary feldspars, are characterized by CF values of 7.8-7.3. In case of olivine abundances the CF values is >8.7 [16]. We used the ACT-React Quick Map to infer the CF map derived from Diviner. Analyses of the Diviner CF map for the examined domes reveals that they do not display the short wavelength CF position characterizes silica-rich lithologies like the Gruithuisen domes. The average CF position of Luther 1 and Hal 1 domes is 8.30 ± 0.1; this value is not significantly different from the average CF position of the typical basaltic maria, which is 8.30-8.40. Hence, the examined domes are not enriched in silica relative to the surrounding mare units and display a classic basaltic composition.

Conclusion

Eight lunar domes, termed C35-C42, have been characterized in their morphometric properties. The domes with higher slopes are C36, C37 and C40 (slope 2.0-2.3°). C39 is the shallower dome with a slope angle of 0.62°. Thus during our lunar domes survey we have classified a total of fifty-six domes in the wide Cauchy shield. A full spectral analysis based on M^3 dataset is in progress. We encourage more high-resolution imagery of this wide lunar region so that we can have more data to identify further lunar domes not characterized in the morphometric and spectral properties yet. Please check also your past imagery and send them to us for the ongoing study (lunar-domes@alpo-astronomy.org).

References

[1] Wilhelms, D. E., 1987. The geologic history of the Moon. USGS Professional Paper 1348.
[2] Head, J. W., & Gifford, A., 1980. Lunar mare domes: classification and modes of origin. The Moon and Planets, 22, 235–257.
[3] Basaltic Volcanism Study Project, 1981. Basaltic Volcanism on the Terrestrial Planets. New York: Pergamon Press.
[4] Lena, R., Wöhler, C., Phillips, J., Chiocchetta, M.T., 2013. Lunar domes: Properties and Formation Processes, Springer Praxis Books.
[5] Lena, R., Lunar domes, chapter in Encyclopedia of Lunar Science Editor: Brian Cudnik, 2015, Springer ISBN: 978-3-319-05546-6.
[6] Lena, R., Magmatic Intrusion Structure, chapter in Encyclopedia of Planetary Landforms Editors: Henrik Hargitai, Ákos Kereszturi, 2015, Springer ISBN: 978-1-4614-3133-6.
[7] Lena, R., Chiocchetta, M. T., Wirths, M., Lazzarotti, P., Phillips, J., Zannelli, C., Buda, S. and Tarsoudis,G., Lunar Domes Atlas http://lunardomeatlas.blogspot.it/ and the Vitruvius Cauchy Quadrant http://vitruviuscauchy.blogspot.it/
[8] Wöhler, C., Lena, R., & Phillips, J., 2007. Formation of lunar mare domes along crustal fractures: Rheologic conditions, dimensions of feeder dikes, and the role of magma evolution. Icarus, 189 (2), 279–307.
[9] Wöhler, C., Lena, R., Lazzarotti, P., Phillips, J., Wirths, M., & Pujic, Z., 2006. A combined spectrophotometric and morphometric study of the lunar mare dome fields near Cauchy, Arago, Hortensius, and Milichius. Icarus, 183, 237–264.
[10] Lena, R., Lazzarotti, P., 2014. Domes in northern Mare Tranquillitatis: Morphometric analysis and mode of formation. Selenology Today, 35, 12-24.
[11] Lena, R., Lazzarotti, P., 2015. Domes in northern Mars Tranquillitatis, near the craters Vitruvius G & M, J. Br. Astron. Assoc. 125, 2, 97-104.
[12] Lena, R., Phillips, J. Lunar domes in the Cauchy shield: Morphometry and mode of emplacement. LPSC 43th, 2012, https://www.lpi.usra.edu/meetings/lpsc2012/pdf/1005.pdf

[13] Lena, R., Phillips, J. Lunar domes in the Cauchy shield: Morphometry and mode of formation. 49th LPSC, 2018, https://www.hou.usra.edu/meetings/lpsc2018/pdf/1005.pdf
[14] Lena, R., Phillips, J. The Cauchy Shield: Morphometric Analysis and Mode of Formation. The Moon (Occasional Papers of the Lunar Section of the British Astronomical Association).Volume 5. November 2017.
[15] Horn, B. K. P., 1989. Height and Gradient from Shading. MIT technical report 1105A. http://people.csail.mit.edu/people/bkph/AIM/AIM-1105A-TEX.pdf
[16] Greenhagen, B.T., Lucey, P. G., Wyatt, M.B., Glotch, T. D., Allen,C.C., Arnold, J. A., Bandfield, J. L., Bowles, N. E., Donaldson Hanna, K. L., Hayne, P. O., Song, E., Thomas, I. R., Paige, D. A., 2010. Global Silicate Mineralogy of the Moon from the Diviner Lunar Radiometer. Science, 329, 1507-1509. doi: 10.1126/science.1192196.